Wavelet-based level set evolution for classification of textured images

Jean-François AUJOL [1,2] & Gilles AUBERT [1] & Laure BLANC-FÉRAUD [2]

[1] Laboratoire J.A.Dieudonné , UMR CNRS 6621
Université de Nice Sophia-Antipolis, Parc Valrose , 06108 Nice Cedex 2 , France

[2] ARIANA, projet commun CNRS/INRIA/UNSA
INRIA Sophia Antipolis, 2004, route des Lucioles, BP93, 06902, Sophia Antipolis Cedex, France

***Abstract*— We present a supervised classification model based on a variational approach. This model is specifically devoted to textured images. We want to get a partition of an image, composed of texture regions separated by regular interfaces. Each kind of texture defines a class. We use a wavelet packet transform to analyze the textures, charactized by their energy distribution in each sub-band. In order to have an image segmentation according to the classes, we model the regions and their interfaces by level set functions. We define a functional on these level sets whose minimizers define the optimal classification according to textures. A system of coupled PDEs is deduced from the functional. By solving this system, each region evolves according to its wavelet coefficients and interacts with the neighbour regions in order to obtain a partition with regular contours. Experiments are shown on synthetic and real images.**

Key-words: Texture, classification, variational approach, level set, active regions, active contours, multiphase, wavelets, PDE.

I. INTRODUCTION

A. Overview

Image classification consists in assigning a label to each pixel of an observed image. This label indicates to which class belongs a pixel. Classification can be seen as a partition problem. This is one of the basic problem in image processing. This concerns many applications as for instance landscape management in teledetection. The classification problem is closely related to the segmentation one, in the sense that the goal is to get a partition of the image composed of homogeneous regions. In the classification problem, each partition represents a class. Many classification models have been developed, especially from regions growing algorithms [1], [2], [3], or by a stochastic approach [4], [5], [6], [7], [8], and most recently by a variational approach [9], [10], [11], [12], [13].

The approach which is used here is inspired from [10], [14], and is based on active contours [9], [15], [16], [17], [18], [19], [20]. The partition we seek is a minimizer of a functional. We compute this minimizer by solving the associated PDE's system. These PDEs guide the interfaces (zero level sets) towards the boundary of the optimal partition thanks to internal (regularity of the interface) and external (data term and partition) forces.

The kind of approach we use ([10], [14]) has the advantage to be faster than the statistical one, whereas the results we get are at least as good as the ones obtained in the statistical approach (as long as the images we deal with are not too much noisy) [21]. Through active contours and PDEs, we can easily introduce regularization constraints on the geometrical shape of the classification regions.

B. Position of our texture model in the existing literature

There exists many models for textured images in the literature [22]. Two main directions emerge:

1) Traditional statistical models, especially Markov random field models (see [4], [7], [5], [8], [6]).
2) Models based on the filtering theory, especially Gabor filters [23], [24], [12] or wavelets [3], [25], [26], [27], [28], [29], [30], [31]. Some of them use the theory of preattentive texture discrimination based on textons [32], [33].

We have chosen to use the wavelets approach which give an excellent way to decompose a signal in different sub-bands in which it is easier to characterize it.

The use of wavelets to analyze textures is not new. There exists mainly two approaches:

1) Models which assume the independence of the distribution of the wavelets coefficients (see [34], [3], [28], [29]).
2) Models which assume a spatial dependence (interactions between the pixels) and through the scales (interactions between the wavelet coefficients through the scales) (see [25], [35], [36], [30], [37], [38], [39], [40]). These models are based on hidden Markov random fields. Their estimation is quite difficult and requires sophisticated algorithm.

We have chosen to use a model of the type proposed by Unser [3]. We consider that a texture is characterized by the energy of its wavelet coefficients in each sub-band of the decomposition. Our choice is confirmed by the quality of the results we get. Our model is new since, as far as we know, it is the only one which uses simultaneously an active contour approach guided by wavelets.

In the existing literature, the closest model is the one proposed by Paragios and Deriche in [12]. However it differs on many points:

1) In [12], the authors use a model presented in [18], and characterize textures with Gabor filters. Historically, Gabor filters have been introduced before wavelet bases (see [41]), but the storage cost is very important, and there exist functions in L^2 which cannot be decomposed into a convergent Gabor coefficients expansion. The construction of wavelet bases by I. Daubechies (see [42]) had overcome these defaults. Moreover, Gabor filters are not orthogonal, which may introduce a significant correlation between coefficients. All these reasons make the use of wavelets more appropriate.
2) The introduction of the active contours in our method is natural: indeed, it comes directly from the functional we seek to minimize. In [12], the energy does not have any coupling terms. They are added in the Euler-Lagrange equations. Moreover, the model in [12] is less general than the one we propose: it only deals with the case of an image having textures dispatched on a textured background. In particular, [12] or [43] show no segmentation or classification result of an image having triple junctions (or more).
3) Let us notice that contrary to the model developed in [10], we do not have a stopping function on the contours: this function was based on the gradient of the image, and as we are interested here with textured images, such an approach is no longer possible. In [12], the authors also use a stopping term on the contours. But to implement it, they need the fact that their model deals with textures components dispatched on a background. In order to keep our classification model the more general as possible, we have decided not to use such a detector of contours. Moreover, it can be checked experimentally that contours do stop without the use of such a stopping function.

Our model is also related to [20], [31], but these approaches deal with image segmentation.

C. Principle of our algorithm

Our classification model is inspired by the work of C. Samson *et al.* who have developed a supervised classification algorithm for non textured images in [10].

The number of classes K present in the image is supposed to be known, as well as the characteristics of each class. If $1 \leq k \leq K$, we will denote by Cl_k the corresponding class. We consider the classification problem as a partition problem and the aim is to get an optimal partition of the image. The domain of the image, Ω, is the union of disjoints sets Ω_k (corresponding to Cl_k). We use a variational level set approach. Each Ω_k is characterized by a level set function Φ_k. The classification is obtained by minimizing a functional with respect to Φ_k with three terms: a partition term, a regularity term, and a data term.

The paper is organized as follows. Section II presents the framework of our classification algorithm using level sets. We need to construct a data term specific to textures. That is why in Section III we give a few precisions about wavelets. We then characterize textures through their wavelet expansion in Section IV. We deduce our data term from this study in Section V, and we present the algorithm we use to minimize it. We then finish by giving some numerical results on both synthetic and real textured images in Section VI.

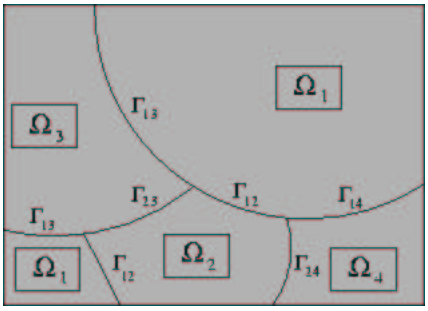

Fig. 1. Classification seen as a partition problem

II. Classification

A. Partition, level set approach

The image is considered as a function $u_0 : \Omega \mapsto \mathbb{R}$ (where Ω is an open subset of $\mathbb{R}^2$). We denote $Cl_k = \{x \in \Omega \,/\, \text{x belongs to the class k}\}$. In order to get a functional formulation rather than a set formulation, we assume that for all $k = 1 \ldots K$, Cl_k is an open set Ω_k given by a Lipschitz function $\Phi_k : \Omega \to \mathbb{R}$ such that:

$$\begin{cases} \Phi_k(x) > 0 & \text{if } x \in \Omega_k \\ \Phi_k(x) = 0 & \text{if } x \in \Gamma_k \\ \Phi_k(x) < 0 & \text{otherwise} \end{cases}$$

(typically, Φ_k is the signed distance function to Γ_k, Φ_k being then lipschitz as soon as Γ_k is lipschitz). Ω_k is thus completely determined by Φ_k (i.e. $x \in \Omega_k \Leftrightarrow H(\Phi_k(x)) = 1$, where H is the Heaviside distribution). The collection of open sets $\{\Omega_k\}$ forms a partition of Ω if and only if $\Omega = \bigcup_k \Omega_k \bigcup_k \Gamma_k$, and if $k \neq l$ $\Omega_k \bigcap \Omega_l = \emptyset$. We denote $\Gamma_k = \partial\Omega_k \bigcap \Omega$ the boundary of Ω_k (except points belonging also to $\partial\Omega$), and $\Gamma_{kl} = \Gamma_{lk} = \Gamma_k \bigcap \Gamma_l$ the interface between Ω_k and Ω_l (see Figure 1).

B. Regularization

We also use the Dirac distribution δ. In order that all the expressions we write have a mathematical meaning, we will use the classical regular approximations of these distributions (see Figure 2):

$$\delta_\alpha(s) = \begin{cases} \frac{1}{2\alpha}\left(1 + \cos\frac{\pi s}{\alpha}\right) & \text{if } |s| \leq \alpha \\ 0 & \text{if } |s| < \alpha \end{cases}$$

$$H_\alpha(s) = \begin{cases} \frac{1}{2}\left(1 + \frac{s}{\alpha} + \frac{1}{\pi}\sin\frac{\pi s}{\alpha}\right) & \text{si } |s| \leq \alpha \\ 1 & \text{if } s > \alpha \\ 0 & \text{if } s < -\alpha \end{cases}$$

When $\alpha \to 0$, we have $\delta_\alpha \to \delta$ and $H_\alpha \to H$ (in the distributional sense).

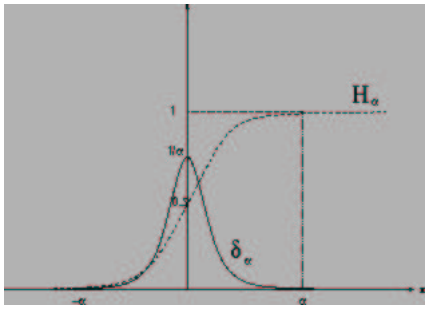

Fig. 2. Approximations δ_α and H_α of the Dirac and Heaviside distributions

C. Functional

Our functional has three terms:

1)

$$F_\alpha^A(\Phi_1,\ldots,\Phi_K) = \lambda \int_\Omega \left(\sum_{k=1}^K H_\alpha(\Phi_i) - 1\right)^2 \quad (2.1)$$

Minimizing this energy term ensures that the result is indeed a partition of the image. It penalizes the pixels which are unclassified ($\sum_{k=1}^K H_\alpha(\Phi_k) = 0$), as well as the ones classified in at least two regions simultaneously ($\sum_{k=1}^K H_\alpha(\Phi_k) > 1$). In fact, to get a partition of Ω, we would need to have $\sum_{k=1}^K H(\Phi_k(x)) = 1\ ,\ \forall x \in \Omega$. We rather minimize the quadratic error, which is easier.

2)

$$F^B(\Phi_1,\ldots,\Phi_K) = \sum_{k=1}^K \gamma_k |\Gamma_k| \quad (2.2)$$

This term penalizes the contours length, which prevent from having too irregulars contours and a lot of small regions. By using the co-area formula, it is possible to show that (the proof is given in [10]):

$$\lim_{\alpha\to 0} \int_\Omega \delta_\alpha(\Phi_k)|\nabla\Phi_k| dx = |\Gamma_k| \quad (2.3)$$

Then, in practice, we seek to minimize:

$$F_\alpha^B(\Phi_1,\ldots,\Phi_K) = \sum_{k=1}^K \gamma_k \int_\Omega \delta_\alpha(\Phi_k)|\nabla\Phi_k| \quad (2.4)$$

3)

$$F^C(\Phi_1,\ldots,\Phi_K) \quad (2.5)$$

This last term stands for the data term, and we will get it from our textures modelization and the maximum likelihood principle (see Section IV).

Complete functional: The functional we want to minimize is the sum of the three previous terms:

$$\begin{aligned} F(\Phi_1,\ldots,\Phi_K) &= F^A(\Phi_1,\ldots,\Phi_K) + F^B(\Phi_1,\ldots,\Phi_K) \\ &\quad + F^C(\Phi_1,\ldots,\Phi_K) \end{aligned} \quad (2.6)$$

III. About wavelets

The texture analysis uses wavelet transform. We refer the interested reader to [44], [42], [41], [34], [45].

A. Undecimated wavelets

The algorithm proposed by S. Mallat [34], [44], [45] gives a non redundant representation of a signal: once the wavelet transformation has been computed, the number of coefficients to store remains the same as for the initial signal. Nevertheless, this algorithm has the drawback to be (a priori) not translation invariant. As the aim of our work is to classify textured images, we want to construct a translation invariant feature. That is why we use wavelet frames (see [3]). The DWF (discrete wavelet frame) corresponds to the DWT (discrete wavelet transform) applied to the input signal with all the possible translations.

B. Wavelet packet transform

A large number of textures can be modelized as quasi-periodic signals (repetition of the same stucture with slight variations) whose dominant frequencies lie in median frequencies channels (see [30]). But the DWT decomposes a signal in a set of channels whose bandwidth is smaller in the low frequency regions. This turns out to be sufficient for regular signals whose information is concentrated at low frequencies, but not for textures. In the case of the DWT, only the low frequency block is redecomposed. To avoid this drawback, we use a wavelet packet transform: this way, each block can be decomposed again.

C. Gray level independence

When an image is decomposed with a wavelet transform or a wavelet packet transform, all the blocks of the decomposition have a zero mean, except the block corresponding to the low frequencies. Its mean corresponds in fact to the mean gray level of the image. But our aim is to classify textured images: the mean of the gray level must not be a feature for a texture. That is why we modify the low frequency block by setting its mean to zero. We get the same kind of results when we simply drop this term.

IV. Texture modelisation

We are now in position to characterize textures through their wavelet decomposition.

A. Idea

We consider that a texture is characterized by the energy of its wavelets coefficients. If we note u_0 the function which represents this texture, we can write (to make things clearer, we use one dimensional notations):

$$u_0 = \sum_n u_{J,n}\phi_{J,n} + \sum_{j=-J}^{-1}\sum_n w_{j,n}\psi_{j,n} \quad (4.7)$$

where ψ is the mother wavelet, ϕ the scaling function and J the order of the decomposition. Thus, we consider that a texture is characterized by the sequence:

$$\left((|u_{J,n}|^2, n\in\mathbb{Z}), (|w_{j,n}|^2, n\in\mathbb{Z}, -J\le j\le -1)\right) \quad (4.8)$$

u_0 is defined over Ω, but we extend it to $\mathbb{R}^2$ by reflection and periodization.

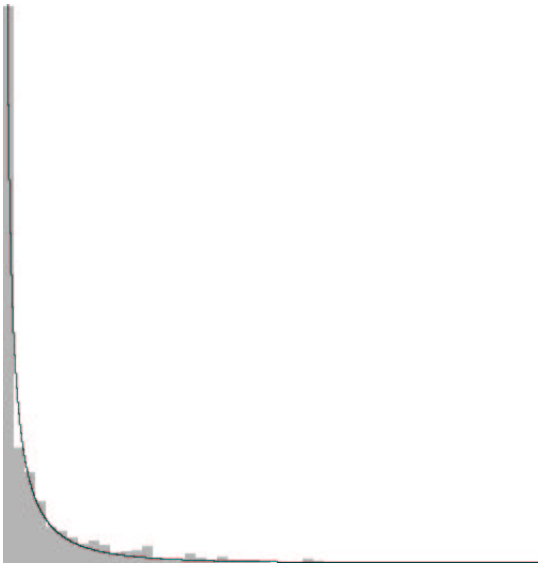

Fig. 3. Theoretical graph of the energy distribution in a sub-band (law (4.10)) and experimental histogram (in a sub-band of the wavelet packet transform of the top right texture of Figure 5) ($\alpha = 40.44$ and $\beta = 1.537$).

B. Probability distribution of the energy

S. Mallat checked experimentally (see [34]) that the distribution of the modulus of the wavelet coefficients in a sub-band of any image follows a generalized gaussian law of the form:

$$p_X(x) = A \exp\left(-\left(\frac{x}{\alpha}\right)^{\beta}\right) \mathbb{I}_{x \geq 0} \tag{4.9}$$

He checked it for the classical wavelet transform, and we made experiments to verify that this still remains true for the wavelet packet transform. As we consider that textures are characterized by their energy, we compute the distribution law of the square of the wavelet coefficients in a sub-band. We get it from (4.9):

$$p_{X^2}(y) = \frac{A}{2\sqrt{y}} \exp\left(-\left(\frac{\sqrt{y}}{\alpha}\right)^{\beta}\right) \mathbb{I}_{y \geq 0} \tag{4.10}$$

This kind of distribution is even pickier than the one given by (4.9). The parameter β modifies the decrease of the pick, and α models the variance. Experimentally, we have checked that the distribution of the energy inside a sub-band is well approximated by a law of this type. Figure 3 shows the probability density function (4.10) effectively match the histogram of the squares of the wavelet packet coefficients in a sub-band. A texture will be charctarized by the parameters α and β in each sub-band.

C. Computation of the parameters of the energy distribution

Our goal is to carry out supervised classification for textured images. "Supervised" means the fact that we know a priori the number of classes which can be found in the image, as well as the parameters of each class. The class parameters α and β can be computed from the first and second order moments of the energy distribution in each sub-band (and we will know these moments). Let us compute these moments.

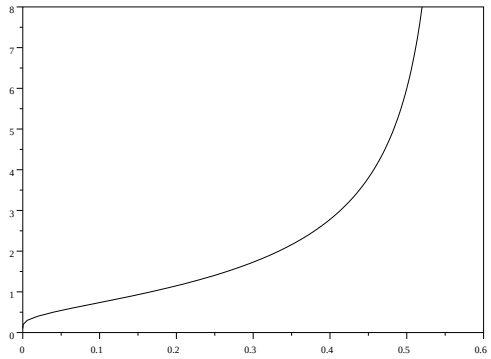

Fig. 4. Graph of F^{-1} (given by (4.17))

Gamma function: The function Γ is defined on $\mathbb{R}_+$ by:

$$\Gamma(t) = \int_0^{+\infty} e^{-u} u^{t-1} du \tag{4.11}$$

By using the fact that $\int_{\mathbb{R}} p_X(x)dx = 1$, we get:

$$A = \frac{\beta}{\alpha \Gamma\left(\frac{1}{\beta}\right)} \tag{4.12}$$

Let us denote $Y = X^2$. We compute the first and second order moments of Y, $M_1 = E(Y)$ and $M_2 = E(Y^2)$, where: $E(Z) = \int_{\mathbb{R}} z\, p_Z(z)dz$. We find:

$$M_1 = E(Y) = E(X^2) = \frac{\alpha^3 A}{\beta} \Gamma\left(\frac{3}{\beta}\right) \tag{4.13}$$

$$M_2 = E(Y^2) = E(X^4) = \frac{\alpha^5 A}{\beta} \Gamma\left(\frac{5}{\beta}\right) \tag{4.14}$$

From (4.13) and (4.14), we get:

$$\alpha = \sqrt{\frac{\Gamma\left(\frac{3}{\beta}\right)}{\Gamma\left(\frac{5}{\beta}\right)} \frac{M_2}{M_1}} \tag{4.15}$$

and $\frac{\Gamma^2\left(\frac{3}{\beta}\right)}{\Gamma\left(\frac{1}{\beta}\right)\Gamma\left(\frac{5}{\beta}\right)} = \frac{M_1^2}{M_2}$. Thus:

$$\beta = F^{-1}\left(\frac{M_1^2}{M_2}\right) \tag{4.16}$$

with:

$$F(x) = \frac{\Gamma^2\left(\frac{3}{x}\right)}{\Gamma\left(\frac{1}{x}\right)\Gamma\left(\frac{5}{x}\right)} \tag{4.17}$$

The graph of F^{-1} is computed numerically and is shown on Figure 4. In practice, $\frac{M_1^2}{M_2}$ ranges over $(0.1, 0.45)$ where F^{-1} is stable.

V. Complete functional

A. Hypotheses

From the modelization we made in the previous section, we now deduce the data term we use in our algorithm. We compute a wavelet packet decomposition of the image (up to the second order in practice): we get I channels ($I = 16$ in practice). We denote by S the set of the pixels of the image.

Definition 5.1. In what follows, we will call the energy at pixel s in S the vector $U(s) = (u_1(s), \dots, u_I(s))$, where $u_i(s)$ is the square of the wavelet coefficient in the sub-band i at pixel s. $u(s)$ will be the texture's feature at pixel s.

Hypotheses:

(H **1)** We assume that, for each texture $k = 1 \dots K$, in each channel $i = 1 \dots I$, the squares of the wavelet packet coefficients follow a law of the type (4.10) of mean $M_1^{k,i}$ and of second order moment $M_2^{k,i}$.

(H**2)** We consider that the different channels are independent. This is an approximation but it allows simple modeling.

As we mentioned before, our goal is to perform supervised classification. The first and second order moments $M_1^{k,i}$ and $M_2^{k,i}$ are assumed to be known by the user.

B. Data term

The goal is to find for each pixel the class which makes the observed energy U the most likely. In other words, we use the *maximum likelihood estimator* for the data term. We want to maximize $P(U|Cl)$, where Cl is the assumed class. In fact, we are going to maximize the log-likelihood, which amounts to minimize, assuming that the conditional probabilities are independant (Cl_s is the assumed class of the pixel s):

$$\begin{aligned} -\ln(P(U|Cl)) &= -\sum_{s\in S} \ln(P(U(s)|Cl_s)) \\ &= -\sum_{k=1}^{K}\sum_{s\in S} \ln(P(U(s)|Cl_s = k))\delta_k(Cl_s) \end{aligned}$$

where $\delta_k(Cl_s) = 1$ if s belongs to the class k, 0 otherwise.

According to our hypotheses (H 1) and (H 2), we have:

$$P(U(s)|Cl_s = k) = \prod_{i=1}^{I} \frac{A_k^i}{2\sqrt{u_i(s)}} \exp\left(-\left(\frac{\sqrt{u_i(s)}}{\alpha_k^i}\right)^{\beta_k^i}\right) \tag{5.18}$$

The parameters A_k^i, α_k^i and β_k^i are computed from the first and second order moments thanks to formulae (4.12), (4.15) and (4.16).

It can now be deduced:

$$-\ln(P(U|Cl)) = \sum_{k=1}^{K}\sum_{i=1}^{I}\sum_{s\in S} B_k^i(s)\delta_k(Cl_s) \tag{5.19}$$

where

$$B_k^i(s) = -\ln A_k^i + \ln 2 + \frac{1}{2}\ln u_i(s) + \left(\frac{\sqrt{u_i(s)}}{\alpha_k^i}\right)^{\beta_k^i} \tag{5.20}$$

To get our fitting term to the data coherent with the two other terms of our functional, and also to simplify notations, we formally write it in a continuous framework:

$$F^C(\Phi_1, \dots, \Phi_K) = \sum_{k=1}^{K}\sum_{i=1}^{I}\int_{\Omega_k} B_k^i(x)dx \tag{5.21}$$

We approximate (5.21) by:

$$F_\alpha^C(\Phi_1, \dots, \Phi_K) = \sum_{k=1}^{K}\sum_{i=1}^{I}\int_{\Omega} H_\alpha(\Phi_k)B_k^i(x)dx \tag{5.22}$$

C. The functional

We are now able to completely write the functional which models the classification problem for textured images:

$$F(\Phi_1, \dots, \Phi_K) = \frac{\lambda}{2}\int_\Omega \left(\sum_{k=1}^{K} H_\alpha(\Phi_k) - 1\right)^2 + \sum_{k=1}^{K}\gamma_k\int_\Omega \delta_\alpha(\Phi_k)|\nabla\Phi_k| + \sum_{k=1}^{K} e_k \sum_{i=1}^{I}\int_\Omega H_\alpha(\Phi_k)B_k^i(x)dx$$

The classical mathematical minimization results do not apply to our functional. Its mathematical study is under investigation (existence and uniqueness of functions $\Phi_1, \dots, \Phi_K$ minimizing our functional).

D. Remark

We have tried other criteria than energy, especially entropy. But in our preliminary trials, energy has proved to be the most interesting criterion. Moreover, in [46], the authors show experimentally that energy is more adapted than entropy for texture features. That is why we have considered energy.

E. Euler-Lagrange Equations

If $\Phi_1, \dots, \Phi_K$ minimize the functional F, then necessarily (if furthermore the $\Phi_1, \dots, \Phi_K$ verify some regularity conditions (see [9] for instance)), we have for $k = 1 \dots K$: $\frac{\partial F}{\partial \Phi_k} = 0$. Assuming that Neumann conditions are verified, the associated Euler-Lagrange equations to F give the following system composed of K-coupled PDE's (see the appendix of [10] for instance): we have for $k = 1 \dots K$

$$0 = \lambda\delta_\alpha(\Phi_k)\left(\sum_{q=1}^{K} H_\alpha(\Phi_q) - 1\right) - \gamma_k\delta_\alpha(\Phi_k)\mathrm{div}\left(\frac{\nabla\Phi_k}{|\nabla\Phi_k|}\right) + e_k\delta_\alpha(\Phi_k)\left(\sum_{i=1}^{I} B_k^i(x)\right) \tag{5.23}$$

F. Dynamical scheme

To solve the PDE's system (5.23), we embed it in the following dynamical scheme ($k = 1 \dots K$):

$$\frac{\partial \Phi_k}{\partial t} = -\delta_\alpha(\Phi_k) \left[\lambda \left(\sum_{q=1}^{K} H_\alpha(\Phi_q) - 1 \right) - \gamma_k \text{div} \left(\frac{\nabla \Phi_k}{|\nabla \Phi_k|} \right) + e_k \left(\sum_{i=1}^{I} B_k^i(x) \right) \right] \quad (5.24)$$

where the initial condition $\Phi_k(0, x)$ is the Euclidean signed distance function to the zero level set Φ_k.

We discretize this system with finite differences (see [10]). We arbitrarily set $\alpha \in \mathbb{R}^+$ (in our experiments, we have used $\alpha = 3.0$). We need to set α small enough so that the approximations of the Dirac and Heaviside distributions (δ_α and H_α) remain reasonable. We also prefer α to be small since the bandwidth on which PDE's (5.24) are not empty depends on it (if $\alpha \in \mathbb{N}$, it contains $2\alpha - 1$ pixels width when ϕ_k is the signed distance to its zero level set). On the contrary, we need α not to be too small so that the band contains enough pixels to compute the different terms of (5.24).

G. Reinitialization

The Φ_k are initialized as Euclidean signed distance functions. Nevertheless, as in the classical active contour method [9]), the evolution of the Φ_k with respect to (5.24) does not keep them as Euclidean signed distance functions to their zero level sets. This prevents the convergence of (5.24) towards some Φ_k minimizing F. That is why it is necessary to periodically reinitialize the Φ_k functions into Euclidean signed distance functions. To do so, we use the PDE:

$$\frac{\partial \Phi}{\partial t} + \text{sign}(\Phi_k)(|\nabla \Phi| - 1) = 0 \quad (5.25)$$

A theoretical study of this PDE, as well as an extension to more general Hamiltonians can be found in [47]. A theoretical proof of the convergence of the algorithm we present here is still under investigation.

VI. Numerical results

A. Choice of parameters

Wavelets: As we explained before, we have chosen in our experiments to use wavelet packet decompositions of the second order to compute the data term. We have tested different kinds of wavelets, and we have chosen to use the Daubechies wavelet with ten vanishing moments (see [42], [44]), this choice appearing to give the best results.

Information given by the user: As the classification is here supervised, the user has to provide the number of classes (textures), as well as the parameters of each class (the first and second order moments of the energy distribution in each sub-band of the wavelet packet decomposition). In our numerical examples, we compute the parameters of each texture from a sample of it. It seems that our method is quite robust with respect to these parameters: changing the sample on which they are computed does not affect the classification result significantly.

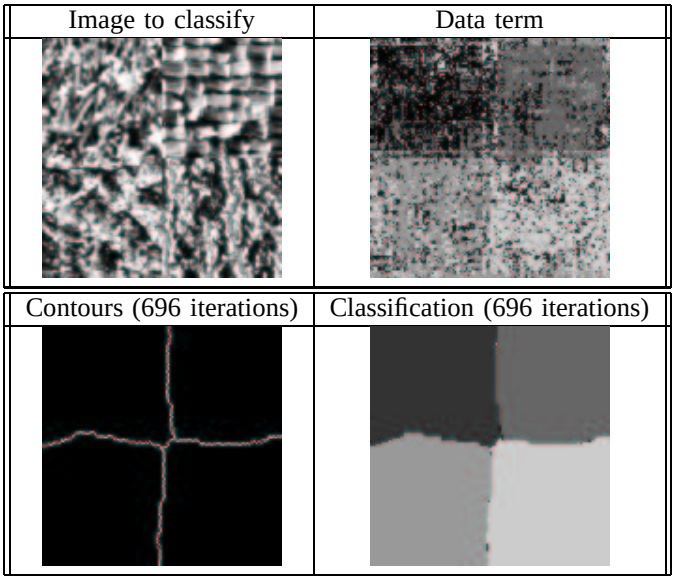

Fig. 5. Classification of a synthetic image composed of four textures

Parameters: In our experiments, we always choose $e_1 = \dots = e_K = 1.0$ and $\gamma_1 = \dots = \gamma_K = \gamma$ ($\gamma \in \mathbb{R}_+$). There remain only two parameters to tune: the partition term coefficient λ, and the common value of the contour regularization terms γ. The parameter λ is first determined with a value large enough in order to ensure at the end of the algorithm that the partition constrainst is satisfied. The results are not sensitive to variations of λ, provided it is large enough. Second, the regularization parameter γ. Variations of γ give more or less regular solutions. This parameter is tuned by trial and error.

Initialization: To get an automatic initialization, and to make it independent of the user, we have then used "seeds": we split the initial image into small sub-images (in practice 5*5 images). In each sub-image, for each class k, we compute the data term by assuming that all the pixels of the sub-image belong to the same class k. We set all the pixels in the sub-image to the class k for which the whole sub-image's energy is the smallest. We have used this initialization in the examples presented here-after.

B. Examples:

In the Figures 5 to 8, we represent the data term by giving to each pixel of the image the class for which its energy is the smallest. This is the classification that we would get if we only used the data term (Maximum Likelihood criterion). Our algorithm is quite fast: for instance, it took us a little more than 4 minutes to process the example of Figure 6 with a processor of 800 MHz and 128 kByte of RAM (the size of the image being 128*128).

1) Synthetic image with four textures: In this example (see figure 5), one sees clearly that our model can handle with triple junctions. On the contrary, as in the classical approach of the Mumford-Shah functional [48], the junction of four textures give two triple junctions in the classified image (at 120 degrees). It is also worth noticing that our algorithm can

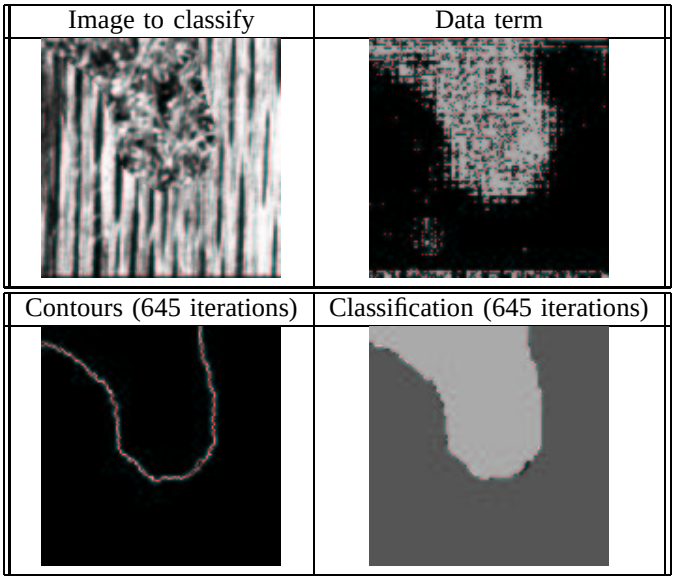

Fig. 6. Classification of a synthetic image composed of two textures

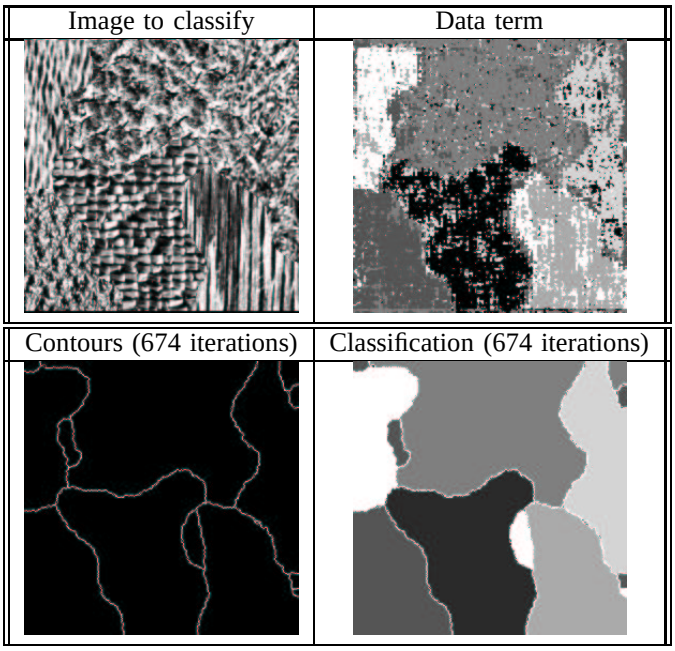

Fig. 7. Classification of a synthetic image with six textures

differentiate these four textures although they are visually very close.

2) Synthetic image with two textures: This example (see figure 6) shows that our model can handle with any kind of geometrical shape (contrary to the model proposed in [13] for instance).

3) Synthetic image with six textures: This example (see figure 7) shows that our model can handle complex textured images. Here, some of the textures are visually very close, and the geometrical shape of the contours are quite well detected. To get more homogeneous classes, we have applied here a Gaussian mask to the data term.

4) Case of a real image with a zebra: This example (see figure 8) also shows that our model can handle with any

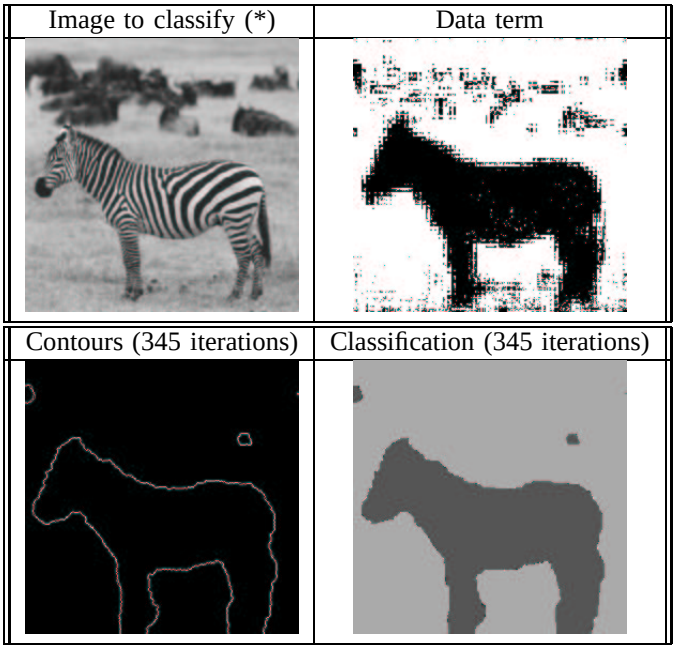

Fig. 8. Classification of a zebra on a background.
(*) Copyright © Corel. All rights reserved.

geometrical shape. The parameters of the background were computed from a sample of grass under the zebra.

VII. Conclusion

We have presented a variational model based on a level set formulation to classify textured images. The proposed algorithm produces segmentation of an entire image according to a priori known texture parameters, by using level sets allowing multiple junctions. The level sets evolve according to wavelet coefficients and interact between each other. The use of level sets enables us to easily introduce constraints on the regions and their contours. It also has the advantage to handle automatically topological changes. In a future work, we plan to do a complete theoretical study of our model, and to combine textured and non textured regions in a single classification process.

References

[1] R. Fjortoft, A. Lopes, P. Marthon, and E. Cubero-Castan, "An optimal multiedge detector for sar image segmentation," *IEE Transactions on Geoscience and Remote Sensing*, vol. 36, no. 3, pp. 793–802, May 1998.

[2] C. Lemarechal, R. Fjortoft, P. Marthon, E. Cubero-Castan, and A. Lopes, "Sar image segmentation by morphlogical methods," in *Proc. SAR Image Analysis, Modelling, and Technique III*. SPIE, September 1998.

[3] M. Unser, "Texture classification and segmentation using wavelet frames," *IEEE Transactions on Image Processing*, vol. 4, no. 11, pp. 1549–1560, November 1995.

[4] M. Berthod, Z. Kato, S. Yu, and J. Zerubia, "Bayesian image classification using markov random fields," *Image and Vision Computing*, vol. 14, no. 4, pp. 285–293, 1996.

[5] C. Bouman and M. Shapiro, "A multiscale random field model for bayesian image segmentation," *IEEE Trans. on Image Precessing*, vol. 3, pp. 162–177, 1994.

[6] S. Lakshmanan and H. Derin, "Simultaneous parameter estimation and segmentation of gibbs random fields using simulated annealing," *IEEE Trans. on Pattern Analysis and Machine Intelligence*, vol. 11, pp. 799–813, August 1989.

[7] B. Manjunath and R. Chellappa, "Unsupervised texture segmentation using markov random fields models," *IEEE Trans. on Pattern Analysis and Machine Intelligence*, vol. 13, pp. 478–482, May 1991.

[8] Z. Kato, "Modélisation markoviennes multirésolutions en vision par ordinateur. application à la segmentation d'images spot," Ph.D. dissertation, Université de Nice Sophia Antipolis, 1994, (in French and English).

[9] G. Aubert and P. Kornprobst, *Mathematical Problems in Image Processing*, ser. Applied Mathematical Sciences. Springer-Verlag, 2002, vol. 147.

[10] C. Samson, L. Blanc-Feraud, G. Aubert, and J. Zerubia, "A level set method for image classification," *IJCV*, vol. 40, no. 3, pp. 187–197, 2000.

[11] ——, "A variational model for image classification and restoration," *IEE Transactions on Pattern Analyis and Machine Intelligence*, vol. 22, no. 5, pp. 460–472, May 2000.

[12] N. Paragios and R. Deriche, "Geodesic active regions and level set methods for supervised texture segmentation," *International Journal of Computer Vision*, vol. 46, no. 3, 2002.

[13] G. Unal, A. Yezzi, and H. Krim, "Information-theoretic active polygons for unsupervised texture segmentation," June 2002, preprint available upon request, submitted.

[14] H.-K. Zhao, T. Chan, B. Merriman, and S. Osher, "A variational level set approach to multiphase motion," *Journal of Computational Physics*, vol. 127, pp. 179–195, July 1996.

[15] V. Caselles, F. Catte, T. Coll, and F. Dibos, "A geometric model for active contours," *Numerische Mathematik*, vol. 66, pp. 1–31, 1993.

[16] M. Sussman, P. Smereka, and S. Osher, "A level set approach for computing solutions to incompressible two-phase flow," *Journal of Computational Physics*, vol. 114, pp. 146–159, 1994.

[17] S. Osher and R. Fedkiw, "Level set methods: An overview and some recent results," *Journal of Computational Physics*, vol. 169, pp. 463–502, 2001.

[18] S. C. Zhu and A.Yuille, "Region competition: unifying snakes, region growing, and bayes/mdl for multi-band image segmentation," *IEEE Transactions on Pattern Analysis and Machine Intelligence*, vol. 18, no. 9, 1996.

[19] T. Chan and L. Vese, "Active contours without edges," *IEEE Transactions on Image Processing*, vol. 10, no. 2, pp. 266–77, February 2001.

[20] L. Vese and T. Chan, "A multiphase level set framework for image segmentation using the Mumford and Shah model," *International Journal of Computer Vision*, vol. 50, no. 3, pp. 271–293, 2002.

[21] C. Samson, L. Blanc-Féraud, G. Aubert, and J. Zerubia, "Two variational models for multispectral image classification," in *Proceedings of the third International workshop on EMMCVPR*, September 2001, sophia Antipolis, France.

[22] T. Young and K. Fu, Eds., *Handbook of Pattern Recognition and Image Processing*. Norman G. Einspruch, 1986.

[23] D. Dunn and W. Higgins, "Optimal gabor filters for texture segmentation," *IEEE Transactions on Image Processing*, vol. 4, no. 7, pp. 947–964, July 1995.

[24] S. Grigorescu, N. Petkov, and P. Kruizinga, "Comparison of textures features based on Gabor filters," *IEEE Trans. on Image Processing*, vol. 11, no. 10, pp. 1160–1167, October 2002.

[25] H. Choi and R. Baraniuk, "Multiscale image segmentation using wavelet-domain hidden markov models," *IEEE Transactions on Image Processing*, vol. 10, no. 9, pp. 1309–1321, September 2001.

[26] C. Bouman, "Multiple resolution segmentation of textured images," *IEEE Transactions on Pattern Analysis and Machine Intelligence*, vol. 13, no. 2, pp. 99–113, July 1995.

[27] N. Fatemi-Ghomi, P. Palmer, and M. Petrou, "Performance evaluation of texture segmentation algorithms based on wavelets," in *Workshop on Performance Characteristics of Vision Algorithms*, April 1996, cambridge.

[28] G. V. de Wouwer, P. Scheunders, and D. V. Dyck, "Statistical texture characterisation from discrete wavelet representation," *IEEE IP*, vol. 8, no. 4, pp. 592–598, 1999.

[29] P. Scheunders, S. Liven, G. V. de Wouwer, P. Vautrot, and D. V. Dyck, "Wavelet-based texture analysis," *International Journal Computer Science and Information management*, December 1997.

[30] T. Chang and C. Kuo, "Texture analysis and classification with tree-structured wavelet transform," *IEEE Transactions on Image Processing*, vol. 2, no. 4, pp. 429–441, October 1993.

[31] G. Koepfler, C. Lopez, and J. Morel, "A multiscale algorithm for image segmentation by variational method," *SIAM Journal of Numerical Analysis*, vol. 31, no. 1, pp. 282–299, February 1994.

[32] B. Julesz, "Texton gradients: The texton theory revisited," *Biological Cybernetics*, vol. 54, pp. 245–251, 1986.

[33] J. Malik and P. Perona, "Preattentive texture discrimination with early vision mecanisms," *Journal of Optical Society of America A*, vol. 7, no. 5, pp. 923–932, May 1990.

[34] S. Mallat, "A theory for multiresolutionsignal decomposition: The wavelet representation," *IEEE Transactions on Pattern Analysis and Machine Intelligence*, vol. 11, no. 7, pp. 674–693, July 1989.

[35] M. Crouse, R. Nowak, and R. Baraniuk, "Wavelet-based statistical signal processing using hidden markov models," *IEEE Transcations on Signal Processing*, vol. 46, no. 4, pp. 886–902, April 1998.

[36] J. Liu and P. Moulin, "Information-theoretic analysis of interscale and intrascale dependencies between image wavelet coefficients," *IEEE Transactions on Image Processing*, vol. 10, no. 11, pp. 1647–1658, November 2001.

[37] J. Chen and A. Kundu, "Rotation and gray scale transform invariant texture identification using wavelet decomposition and hidden markov model," *IEEE Transactions on Pattern Analysis and Machine Intelligence*, vol. 16, no. 2, pp. 208–214, February 1994.

[38] D. Leporini and J. Pesquet, "Bayesian wavelet denoising: Besov priors and non-gaussian noises," *Signal Processing*, vol. 81, pp. 55–67, 2001.

[39] H. Choi and R. Baraniuk, "Multiple basis wavelet denoising using besov projections," in *ICIP*, vol. 1, 1999, pp. 595–9.

[40] ——, "Information-theoretic interpretation of besov spaces," in *SPIE*, August 2000.

[41] Y. Meyer, "Oscillating patterns in image processing and in some nonlinear evolution equations," March 2001, the Fifteenth Dean Jacquelines B. Lewis Memorial Lectures.

[42] I. Daubechies, *Ten lectures on wavelets*. SIAM, 1992.

[43] N. K. Paragios, "Geodesic active regions and level set methods: Contributions and applications in artificial vision," Ph.D. dissertation, University of Nice Sophia Antipolis, January 2000.

[44] S. Mallat, *A Wavelet Tour of Signal Processing*. Academic Press, 1998.

[45] ——, "Multiresolution approximations and wavelet orthonormal bases of $l^2(r)$," *Transactions of the American Mathematical Society*, vol. 315, no. 1, pp. 69–87, September 1989.

[46] A. Laine and J. Fan, "Texture classification by wavelet packet signatures," *IEEE Trans. on Pattern Analysis and Machine Intelligence*, vol. 11, pp. 1186–1190, 1993.

[47] G. Aubert and J. Aujol, "Signed distance functions and viscosity solutions of discontinuous Hamilton-Jacobi equations," July 2002, iNRIA Research Report 4507.

[48] D. Mumford and J. Shah, "Boundary detection by minimizing functionals," in *Proc. IEEE Conf. on Computer Vison and Pattern Recognition*. SPIE, 1985, san Francisco.